THE JOURNAL OF BIOLOGICAL CHEMISTRY VOL. 282, NO. 42, pp. 30776–30784, October 19, 2007

Single Molecule Imaging of Tid1/Rdh54, a Rad54 Homolog That Translocates on Duplex DNA and Can Disrupt Joint Molecules*[S]

Received for publication, June 11, 2007, and in revised form, August 13, 2007 Published, JBC Papers in Press, August 16, 2007, DOI 10.1074/jbc.M704767200

Amitabh V. Nimonkar[‡§], Ichiro Amitani[‡§], Ronald J. Baskin[§], and Stephen C. Kowalczykowski[‡§1]

From the [‡]Section of Microbiology and [§]Section of Molecular and Cellular Biology, University of California, Davis, California 95616

The *Saccharomyces cerevisiae* Tid1 protein is important for the recombinational repair of double-stranded DNA breaks during meiosis. Tid1 is a member of Swi2/Snf2 family of chromatin remodeling proteins and shares homology with Rad54. Members of this family hydrolyze ATP and promote 1) chromatin remodeling, 2) DNA topology alterations, and 3) displacement of proteins from DNA. All of these activities are presumed to require translocation of the protein on DNA. Here we use single-molecule visualization to provide direct evidence for the ability of Tid1 to translocate on DNA. Tid1 translocation is ATP-dependent, and the velocities are broadly distributed, with the average being 84 ± 39 base pairs/s. Translocation is processive, with the average molecule traveling ~10,000 base pairs before pausing or dissociating. Many molecules display simple monotonic unidirectional translocation, but the majority display complex translocation behavior comprising intermittent pauses, direction reversals, and velocity changes. Finally, we demonstrate that translocation by Tid1 on DNA can result in disruption of three-stranded DNA structures. The ability of Tid1 translocation to clear DNA of proteins and to migrate recombination intermediates may be of critical importance for DNA repair and chromosome dynamics.

The *TID1* (two-hybrid interacting with Dmc1) (1) gene product, also known as *RDH54* (Rad homolog 54), is required for mitotic as well as meiotic recombination (2, 3). Tid1 participates in mitotic recombinational repair of double-stranded DNA (dsDNA)[2] breaks via a minor pathway that does not require Rad54 (3). However, Tid1 plays a much more important role during meiotic recombination, since *tid1* mutants exhibit poor sporulation and reduction in spore viability (2). Meiotic recombination is initiated by the infliction of programmed "cuts" in the chromosome (4, 5). These dsDNA breaks are processed to generate 3′-tailed single-stranded DNA (ssDNA), upon which a class of proteins called DNA strand exchange proteins assemble to form nucleoprotein filaments (6). These nucleoprotein filaments represent the active species during recombination and have the ability to scan DNA molecules in *trans*, locate a region of DNA sequence homology, and mediate DNA pairing. This reaction is called DNA strand invasion (6) and is mediated by Dmc1 and Rad51 (7), the two RecA homologs encoded by *Saccharomyces cerevisiae* (8, 9).

The process of template-directed DNA repair involves many additional proteins. One class of such proteins is the DNA translocases, motor proteins that can translocate on duplex DNA and remove impediments. Meiotic yeast cells possess two homologous DNA translocases that are involved in recombination: Tid1 and Rad54 (3). It is speculated that Tid1 primarily cooperates with Dmc1 to promote interhomolog DNA strand exchange, whereas Rad54 would function with Rad51 to promote intersister DNA strand exchange (3, 10, 11). Because DNA synthesis is needed to replicate the information that is lost during the processing of the DNA ends, the activity of DNA translocases may play a crucial role in clearing the DNA strand exchange proteins from the newly formed DNA heteroduplex, thereby making the 3′-end of the invading ssDNA accessible to the polymerase (12). Rad54 will also stimulate the branch migration of this 3-stranded pairing intermediate (13, 14). Finally, capture of the second end of the dsDNA break (15), followed by branch migration generates a pair of Holliday junctions. The Holliday junction is a symmetric four-way DNA structure that can undergo branch migration, and recently, Rad54 was shown to promote such migration, a process that increases or decreases the extent of DNA heteroduplex (16). Thus, it is evident that dsDNA translocases are multifaceted proteins playing important roles during both early and late steps of homologous recombination.

Tid1 and Rad54 belong to the Swi2/Snf2 family of chromatin-remodeling proteins (17). Members of this family were inferred to be ATP-dependent duplex DNA translocases, and recent single molecule observations have provided the most direct evidence for translocation (18–20). Rad54 performs a wide variety of functions potentially important to recombinational DNA repair: alteration of DNA topology (10), displacement of Rad51 from dsDNA (21), stimulation of DNA pairing by Rad51 on both naked DNA (22, 23) and chromatin (24, 25), and catalysis of nucleosome sliding on DNA (26). Each of these activities is presumably a consequence of the ability of the pro-

* This work was supported by National Institutes of Health Grants GM-62653 and GM-64745 (to S. C. K.). The costs of publication of this article were defrayed in part by the payment of page charges. This article must therefore be hereby marked "*advertisement*" in accordance with 18 U.S.C. Section 1734 solely to indicate this fact.

[S] The on-line version of this article (available at http://www.jbc.org) contains supplemental Movies M1–M4.

[1] To whom correspondence should be addressed: University of California, Section of Microbiology, One Shields Ave., Briggs Hall, Rm. 310, Davis, CA 95616-8665. Tel.: 530-752-5938; Fax: 530-752-5939; E-mail: sckowalczykowski@ucdavis.edu.

[2] The abbreviations used are: dsDNA, double-stranded DNA; ATPγS, adenosine 5′-*O*-(3-thiotriphosphate); D-loop, displacement loop; FITC, fluorescein isothiocyanate; GST, glutathione *S*-transferase; nt, nucleotide(s); ssDNA, single-stranded DNA.

tein to actively translocate on dsDNA. Notably, because Rad54 translocates on dsDNA and not on ssDNA, as is the case for DNA helicases (27), it does not separate dsDNA into its component DNA strands.

Given the fact that Tid1 is a structural (37% amino acid sequence similarity) and functional relative of Rad54 (1–3, 17), it might be expected to possess similar functional characteristics. Indeed, Tid1 demonstrates strong ATPase activity and can alter DNA topology (11). To determine whether Tid1 can translocate on DNA as well, we visualized individual Tid1 molecules on single DNA molecules. Here we show that Tid1, like its homolog Rad54, can translocate on dsDNA in an ATP-dependent manner (20). Our observations are in agreement with and complement those in a recent study that appeared while our manuscript was in preparation (28). In addition, our study shows that Tid1 can "unwind" three-stranded DNA structures by virtue of its ability to translocate on DNA, thereby establishing that Tid1 can act on intermediates of recombination. Our finding is consistent with the reported ability of Rad54 to disrupt triple helical structures (25). The single molecule detection of movement reported here permits quantification of translocation, as well as visualization of complex behavior, that cannot be uncovered by ensemble measurements. The similarity of translocation behavior exhibited by Tid1 and Rad54 suggests that each performs a similar biological function but that functional differentiation arises from the specific interaction with the respective DNA strand exchange protein, Dmc1 or Rad51.

EXPERIMENTAL PROCEDURES

Cloning and Purification of GST-Tid1—The full-length *TID1* gene was cloned into an expression vector (pWDH597; kind gift from Dr. W.-D. Heyer, University of California, Davis), such that it was in frame and downstream of a glutathione *S*-transferase (GST) tag. The recombinant protein is therefore 130.6 kDa (26.5-kDa GST and 104.1-kDa Tid1). The expression construct was designed in a way that introduces a thrombin cleavage site between GST and Tid1 (14). The recombinant protein was expressed in yeast; we recovered ~2 mg of protein starting from 20 g of cells. The GST-Tid1 fusion protein was purified to homogeneity using a two-column purification scheme similar to the one employed to purify Rad54 (29). The purity of the protein was estimated to be >95%, as determined by SDS-polyacrylamide gel electrophoresis and staining with Coomassie Brilliant Blue. The concentration of the protein was determined spectrophotometrically using an extinction coefficient of 106,800 M^{-1} cm^{-1} at 280 nm. The purified fusion protein is a dsDNA-dependent ATPase, with V_{max} and K_m[3] comparable with published values (11). The k_{cat} values of Tid1 with and without tag were identical,[4] indicating that the tag does not interfere with Tid1 biochemical function. The details of purification and biochemical characterization of GST-Tid1 will be published elsewhere.[3]

Proteins and Nucleic Acids—RecA was purified as described (30). T4 DNA ligase, T4 polynucleotide kinase and AatII were purchased from New England Biolabs. Proteinase K was purchased from Roche Applied Science. A 100-mer oligodeoxyribonucleotide, complementary to nucleotides 2451–2550 of the minus strand of pUC19, was purchased from Sigma Genosys and gel-purified on a 12% denaturing polyacrylamide gel. The 100-mer was 5′-^{32}P-labeled using T4 polynucleotide kinase and [γ-^{32}P]ATP (4,500 Ci/mmol; PerkinElmer Life Sciences) and purified using MicroSpin G-25 columns (GE Healthcare). Supercoiled pUC19 DNA was purified by nonalkaline lysis followed by $CsCl_2$ density gradient centrifugation (31). DNA concentrations of the 100-mer and pUC19 (2,686 bp) are expressed in moles of nucleotides (nt) as well as molecules, using molar extinction coefficients at 260 nm of 9.98×10^3 and 6.6×10^3 M^{-1} cm^{-1}, respectively.

Preparation of Fluorescein Isothiocyanate (FITC)-Tid1-DNA-Bead Complexes—The DNA-bead complexes were made as described (20). Subsequently, the FITC-Tid1-DNA-bead complex was assembled by mixing 10 nM Tid1 with 25 pM DNA-bead complex, followed by the addition of 670 nM anti-GST antibody, labeled with FITC (Immunology Consultants Laboratory; average labeling ~6 fluorophores/antibody) in phosphate-buffered saline solution containing 0.2% bovine serum albumin. The mixture was incubated at room temperature for 10 min and transferred to 400 μl of a degassed solution containing 40 mM Tris acetate, pH 8.2, 30 mM dithiothreitol, and 15% sucrose. The binding of the antibody to Tid1 (hereafter referred to as FITC-Tid1) reduces the dsDNA-dependent ATPase activity by ~40–60% and correlated with a reduction in the amount of FITC-Tid1 capable of binding to dsDNA as measured by electrophoretic mobility shift assays (data not shown); we conclude that the antibody prevents these Tid1 molecules from binding to the DNA. Since we select for only DNA-bound Tid1 complexes, the inhibitory effect of the antibody does not influence our single molecule analysis.

Single Molecule Tid1 Translocation Assay—The FITC-Tid1-DNA-bead complex was introduced into the first channel of a multichannel flow cell. The flow cell was held on a temperature-controlled motorized sample stage, mounted on an inverted microscope (Nikon TE2000U). The FITC-labeled Tid1-DNA-bead complex was excited with an argon laser (Spectra-Physics 161C-030; 488 nm) using the appropriate filter set and imaged with an EB-CCD camera (C7190-23; Hamamatsu Photonics, Hamamatsu, Japan). The images were recorded on S-VHS tape. Translocation of Tid1 along dsDNA was initiated by moving the trapped FITC-Tid1-DNA-bead complex to the second channel of the flow cell containing a degassed solution of 40 mM Tris acetate, pH 8.2, 30 mM dithiothreitol, 15% sucrose, 2 mM magnesium acetate, and 1 mM ATP. The linear flow rate at the trap position was 120 μm/s.

Data Analysis—Data analysis was performed largely as described (20) with the following exceptions. Images were digitized using a frame grabber controlled by ImageJ (version 1.345). The position of the FITC-Tid1 complex was determined by fitting the fluorescent intensity distribution to a two-dimensional Gaussian function,

$$f(x, y) = A \times \exp\left(-\frac{(x - x_c)^2}{S_x^2} - \frac{(y - y_c)^2}{S_y^2}\right) + B \quad \text{(Eq. 1)}$$

The length of the λ DNA was measured under identical condi-

[3] A. V. Nimonkar and S. C. Kowalczykowski, manuscript in preparation.
[4] A. V. Nimonkar and S. C. Kowalczykowski, unpublished observations.

tions by using DNA that was end-labeled with a fluorescent tag; the tag comprised a chemically synthesized oligonucleotide (Operon) containing digoxigenin that was ligated to the end of λ DNA opposite the bead attachment end, to which sheep anti-digoxigenin antibody (Roche Applied Science) was bound and to which Cy3-labeled anti-sheep IgG (Chemicon) was bound. The position of the end label was determined as above, and the distance (*i.e.* length) to the bead in the optical trap (whose position was determined by visual inspection) was obtained. For the FITC-Tid1 translocation measurements, the distance, *D*, between the bead and FITC-Tid1 was calculated using Equation 2.

$$D = \sqrt{(x_{\text{Tid1}} - x_{\text{bead}})^2 + (y_{\text{Tid1}} - y_{\text{bead}})^2} \qquad \text{(Eq. 2)}$$

Generation of Three-stranded DNA Structures—Displacement loops (D-loops) were formed using RecA as follows: 5′-^{32}P 100-mer (0.9 μM nt; 9 nM molecules) was preincubated with RecA (0.3 μM) in a buffer containing 25 mM Tris acetate, (pH 7.5), 10 mM magnesium acetate, 1 mM dithiothreitol, 2.5 mM ATPγS, and 100 μg/ml bovine serum albumin for 5 min at 37 °C. The reaction was supplemented with pUC19 Form I DNA (48 μM nt; 9 nM molecules) and further incubated for 5 min at 37 °C. The reaction was deproteinized using the Promega Wizard DNA clean-up system, followed by removal of excess unreacted oligonucleotide by gel filtration through a Chroma Spin + TE-1000 column (BD Biosciences). To determine the yield of D-loop formation, a fraction of the RecA-catalyzed D-loop reaction was analyzed by electrophoresis in 0.8% agarose gel (4.5 V/cm for ~1 h). Following electrophoresis, the gels were dried on DE81 paper (Whatman), analyzed, and quantified using a Molecular Dynamics Storm 860 PhosphorImager (GE Healthcare); the yield of D-loops was ~35–40%. The DNA concentration was ~15 μM nt (~3 nM molecules).

Linear joint molecules were formed by mixing AatII-linearized pUC19 (0.9 μM nt; 9 nM molecules) with 5′-^{32}P 100-mer (48 μM nt; 9 nM molecules) in a buffer containing 10 mM Tris, 1 mM EDTA, 100 mM NaCl. AatII cuts pUC19 at residue 2617. The reaction mixture was heated to 95 °C for 5 min and gradually cooled to room temperature to allow formation of linear joint molecules (5–6 h). Since the 100-mer is complementary to residues 2451–2550, annealing of the 100-mer to AatII-linearized pUC19 would generate a three-stranded flapped structure at the end (see schematic diagram in Fig. 6*D*). The free 100-mer was removed by gel filtration through a Chroma Spin + TE-1000 column. The yield was ~35–40% and was determined as described for D-loop formation. The DNA concentration was ~10 μM nt (~2 nM molecules).

Dissociation of D-loops and Linear Joint Molecules by Tid1—Dissociation reactions with joint molecules and Tid1 were performed in a buffer containing 25 mM Tris acetate (pH 7.5), 10 mM magnesium acetate, 1 mM dithiothreitol, 2.5 mM ATP, and 100 μg/ml bovine serum albumin. Reactions were incubated at 30 °C and terminated by the addition of termination buffer (final concentration: 2% SDS, 3 μg/μl proteinase K, 50 mM EDTA; incubation time 20 min). Reaction products were analyzed by electrophoresis in 0.8% agarose gel (4.5 V/cm for ~1 h). Following electrophoresis, the gels were dried on DE81 paper (Whatman), analyzed, and quantified using a Molecular Dynamics Storm 860 PhosphorImager (GE Healthcare).

RESULTS AND DISCUSSION

Tid1 Translocates on dsDNA—To visualize translocation of Tid1 on DNA, we adopted the strategy used previously for Rad54 (20). This involved purification of a functional protein fusion of GST and Tid1. The N-terminal GST tag provides an excellent tool to visualize the protein using an anti-GST antibody to which fluorescent dye is conjugated. Consequently, anti-GST antibody, labeled with FITC, was used to visualize GST-Tid1 (hereafter referred to as FITC-Tid1). The FITC-Tid1 complex was subsequently used to image translocation on individual DNA molecules. The instrumentation, consisting of an epifluorescence microscope, an optical trap, and a multichannel flow cell, was essentially as described previously (20, 32). Briefly, a bacteriophage λ DNA molecule was biotinylated at one end and attached to a 1-μm streptavidin-coated polystyrene bead (Fig. 1*A*). The DNA-bead complex was incubated with FITC-Tid1 in the absence of ATP to allow binding to DNA but not translocation. The bound FITC-Tid1-DNA-bead complex was introduced in the first channel of a two-channel flow cell. The laminar flow in the multichannel flow cell maintains a boundary between the channels, which limits mixing of solutions. The enzyme-bead-DNA complex was captured by a laser trap in the first channel, thereby tethering one end of the DNA molecule. The trapped DNA molecule was subsequently moved to the second channel of the flow cell, which contained ATP. Introduction of FITC-Tid1 into the ATP solution initiates translocation on the DNA tethered to the bead. Because the second flow channel lacked free protein as well as antibody, additional binding or rebinding cannot occur, and background fluorescence from free FITC-Tid1 is nonexistent. The FITC-Tid1 complex on DNA was imaged using a CCD camera attached to the fluorescence microscope and recorded on analog video tape. In the current instrument, flow is from right to left. Movement of the FITC-Tid1 toward the bead (opposite to the direction of flow) is called "upstream," whereas movement away from the bead (in the direction of flow) is called "downstream."

We observed that translation of the FITC-Tid1-DNA-bead complex into the ATP-containing channel initiated translocation of the FITC-Tid1 along the dsDNA (Fig. 1*A*). Individual frames from two different videos show, in one case, a fluorescent FITC-Tid1 complex moving downstream (*left side*) away from the bead in the optical trap (which is also fluorescent due to nonspecific binding of the FITC-antibody to the bead) (20), and a second example moving in the upstream direction (*right side*) toward the bead. The DNA molecule is invisible, because it is not labeled. The intensity of FITC-Tid1 is seen to decrease over time due to photobleaching of the fluorescent dye molecules. Translocation of the FITC-Tid1 is readily displayed by stacking video image "slices," each containing an image segment through only the bead and moving protein, for successive video frames to produce a kymograph. Fig. 1*B* shows the lateral position of the FITC-Tid1 as a function of time, clearly demonstrating downstream (*left*) as well as upstream (*right*) movement on λ DNA.

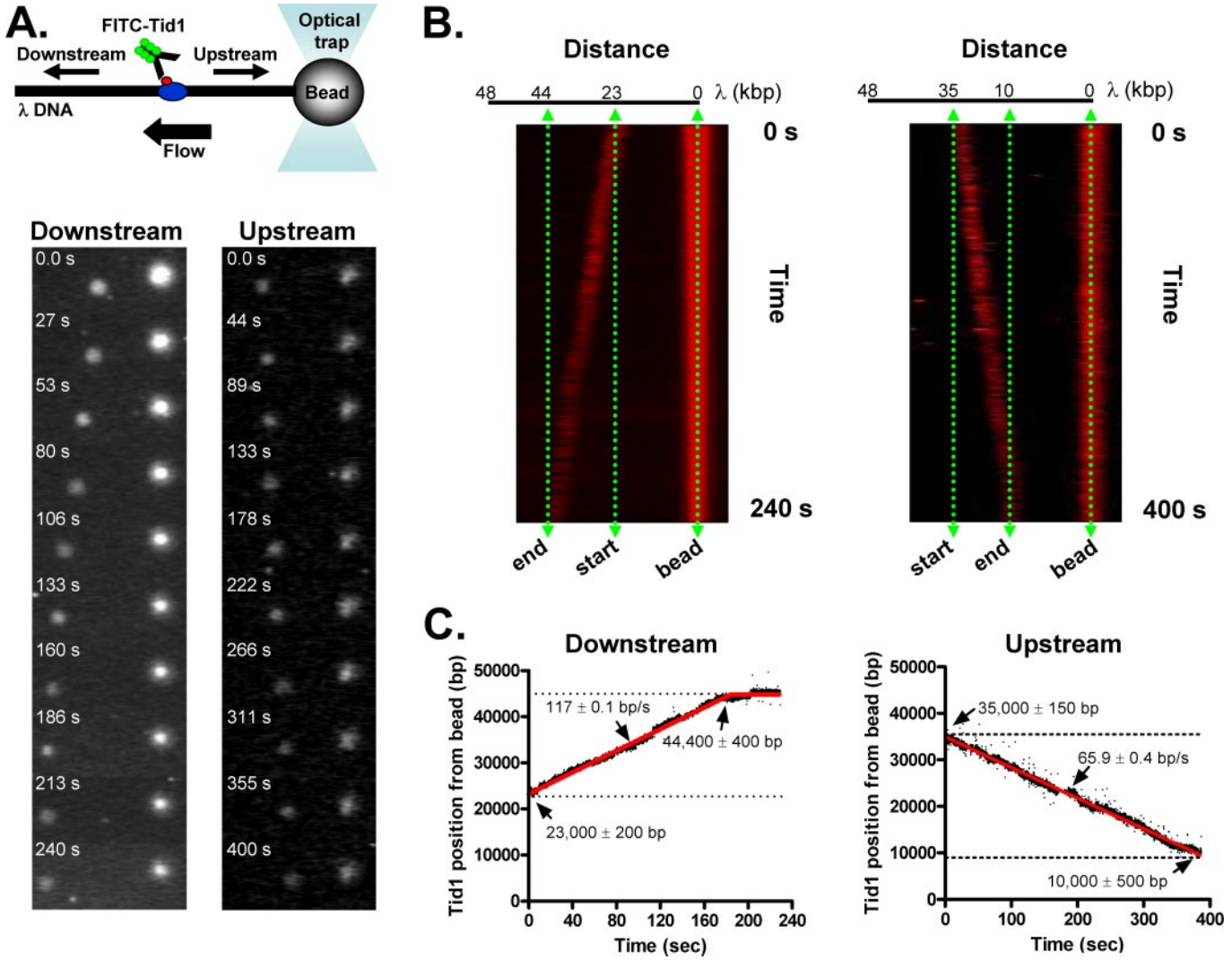

FIGURE 1. **Tid1 translocates on dsDNA.** *A*, a schematic illustration of the optically trapped DNA-bead complex with bound FITC-Tid1 complex. Sequential images of Tid1 translocation in the downstream (*vertical strip* on the *left*) and upstream (*vertical strip* on the *right*) direction are shown *below* the illustration. The time for every frame is indicated. (See movies M1 and M2 for the videos). *B*, kymographs depicting downstream (in the direction of flow) and upstream (in the direction opposite of flow) translocation of Tid1 on dsDNA. The *vertical green arrows* mark the initial binding site of FITC-Tid1 (start), the position of the molecule after translocation (*end*), and the position of the bead (*bead*). A schematic of the λ DNA is drawn at the *top* of the kymographs. *C*, graphical representations of downstream and upstream translocation of Tid1 on dsDNA. The position of Tid1 relative to the bead was plotted as a function of time. The translocation profiles were fit using Prism version 4 to a two-segment line for downstream translocation and to a single segment line for upstream translocation. The initial and final positions and velocities of translocation, along with their respective S.D. values, are indicated.

To determine the velocity of translocation as well as the distance traveled by the translocating complex, its position relative to the trapped bead was plotted as a function of time (Fig. 1*C*). In the case of the downstream translocating complex (*left*), the FITC-Tid1 complex initially bound approximately in the middle of the λ DNA at 23,000 ± 200 bp and then translocated downstream monotonically for almost 21 kbp to the end of the DNA molecule. The velocity of translocation was 117 ± 0.1 bp/s.

For the example of the FITC-Tid1 that moved upstream along the DNA (Fig. 1, *A* and *B*, *right panels*), this molecule initially bound to the DNA at about 35,000 ± 150 bp from the bead (Fig. 1*C*, *right*). It translocated upstream monotonically at a rate of 66 ± 0.4 bp/s, for a distance of about 25 kbp. Although the downstream translocation by FITC-Tid1 can be explained by flow-induced movement, the upstream translocation cannot; however, as will be established below, translocation is ATP-dependent and of comparable magnitude in either direction. Thus, Tid1 clearly has the capacity to translocate on dsDNA.

Tid1 Exhibits a Lower Translocation Velocity and Processivity than Rad54—For the collection of molecules visualized (n = 21), we observed that 40% of the FITC-Tid1 moved initially in the upstream direction, and the remainder moved in the downstream direction (Table 1). Furthermore, although many showed the simple behavior displayed in Fig. 1, most molecules showed a change in velocity during translocation, which is discussed below. A histogram of all translocation velocity segments (40 segments in total for the 21 molecules) shows an approximately Gaussian distribution (Fig. 2*A*); a similar distribution is obtained when only the initial velocity segments (n = 21) are used (data not shown). The distribution may be bimodal, but the small sample size prevents us from making an unequivocal statement about the nature of the distribution. Fit-

ting the data to a single Gaussian (*red line*) yields a mean velocity of 84 ± 39 bp/s, whereas fitting the data to a bimodal Gaussian yields two peaks with mean velocities of 73 ± 43 and 144 ± 51 bp/s; although interesting, it is unclear whether the 2-fold difference in mean velocities is meaningful. Regardless of the nature of the distribution, there was no experimentally significant bias in the velocity distribution for molecules that moved upstream *versus* those that moved downstream (a difference of ~15 bp/s; data not shown), as was also the case for Rad54 (20). These mean values are ~2–4-fold lower than the translocation velocity of Rad54 (302 ± 22 bp/s), which was determined using the same technique. As for Rad54 (20) (and RecBCD (32)), the Tid1 translocation velocities were seen to vary as much as 10-fold between the fastest and the slowest molecule due to an as yet undefined intrinsic molecular heterogeneity.

Next, we determined the average distance translocated by FITC-Tid1 molecules. Traditionally, processivity is defined as the distance traveled, or the number of times that an enzyme acts, before dissociating from the substrate (33). Due to the complex translocation trajectories observed for FITC-Tid1, several definitions of processivity can be considered. The first is to consider only the molecules that showed simple monotonic behavior; this method, unfortunately, represents only seven molecules (Table 1). For these seven, the distances traveled ranged from 3,450 to 23,800 bp, with a mean of ~15,000 bp. Due to the small size of this sample and our analysis below, which suggests that each translocation segment of complex behavior represents the action of a different motor in the complex, we measured the distance of each translocation segment where an FITC-Tid1 moved at a uniform velocity without detectable pausing, reversing, or changing velocity. To determine the processivity of FITC-Tid1 translocation, the fraction of molecules that translocated at least the distance indicated on the *x* axis was plotted (Fig. 2*B*); it should be noted that values below ~2,000 bp are underrepresented, because molecules traveling those short distances are not easily counted due to detection limits. The processivity parameter, *P*, is defined as the probability of a bound molecule translocating one DNA lattice position, assumed to be a base pair, relative to the probability of it dissociating (33); thus, the probability of any FITC-Tid1 molecule advancing at least *n* base pairs is given by P^n. At and above 2,000 bp translocated, the experimental distribution can be fit to this power function (red line) to yield a value for *P* of 0.9999 ($\pm 1 \times 10^{-5}$). The average distance of translocation, *N*, calculated using $N = 1/(1 - P)$, is ~10,000 bp (33), which is comparable with the average distance traveled by the simply behaving FITC-Tid1 molecules. Using the same methods of analysis, our results demonstrate that, compared with Rad54 ($N \approx 14{,}000$ bp) (20), Tid1 is a slower (~2–4-fold) and slightly less processive translocase.

TABLE 1
Distribution of Tid1 translocation characteristics

The behaviors of the FITC-Tid1 translocation complexes are expressed as percentages. A total of 21 translocating complexes were analyzed. The actual distributions are as follows: seven of 21 showed simple translocation, of which four showed downstream and three showed upstream translocation; 14 of 21 showed complex translocation, of which four demonstrated intermittent pausing, five showed translocation reversals, and all 14 exhibited multiple velocities. The percentages for the three types of complex behavior do not sum to 100%, because the translocation characteristics overlapped (*e.g.* a bidirectional complex also displayed multiple velocities) (*e.g.* Fig. 4).

Translocation	Behavior
Simple (33%)	Upstream only (40%) Downstream only (60%)
Complex (66%)	Intermittent pausing (28%) Direction change (36%) Multiple velocities (100%)

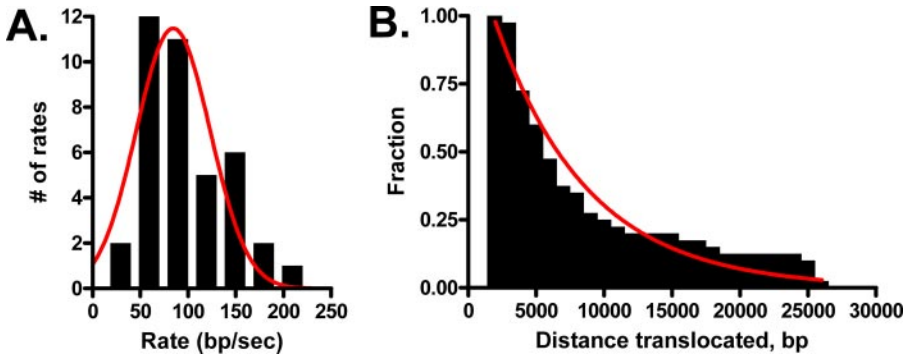

FIGURE 2. **Frequency distribution of translocation rate and distance traveled by Tid1.** *A*, distribution of Tid1 translocation velocities assigned to 30 bp/s intervals. Each value ($n = 40$) represents the rate of a translocation trajectory segment during which the molecule displayed no detectable pause, direction change, or velocity alteration. The *red line* represents a fit of the rates to a Gaussian distribution. *B*, the fraction of Tid1 molecules that traveled at least the distance indicated without pausing or changing direction or velocity were binned into 1,000-bp intervals and plotted as a function of traveled distance. kbp were determined by fitting the data to $Y = P^n$ (*red line*), where *Y* is the fraction of translocating molecules that traveled at least the distance indicated, and *n* is the distance translocated in bp; *P* is 0.9999.

FITC-Tid1 Translocation Requires ATP—Mutations in the Walker motif render Rad54 and Tid1 inactive, thereby indicating a requirement for ATP (11, 26, 34). Indeed, Rad54 translocation was shown to be dependent on ATP (20). We therefore tested the requirement for ATP during Tid1 translocation. For this experiment, we used a three-channel flow cell (35). The additional channel allowed us to study the behavior of a captured complex in two different solutions (namely reaction buffer containing ATP and the same buffer without ATP). Fig. 3*A* shows a FITC-Tid1 bound to DNA that was captured in the first channel as described earlier and moved to the second channel lacking ATP. The initial binding position of FITC-Tid1 on DNA was 15,900 ± 500 bp (Fig. 3*B*). The molecule was observed for 50 s, with continued buffer flow, during which time the Tid1 complex remained stationery, further demonstrating that flow alone is insufficient to move FITC-Tid1. The molecule was then moved to the third channel that contained ATP. As seen in the kymograph (Fig. 3*A*), Tid1 began translocating immediately upon being translated to the ATP-containing solution. Translocation was monitored for ~100 s, during which the Tid1 complex traveled a distance of ~4,000 bp at a constant rate of 42.7 ± 0.2 bp/s (Fig. 3*B*, *red line*). To provide further evidence that the movement

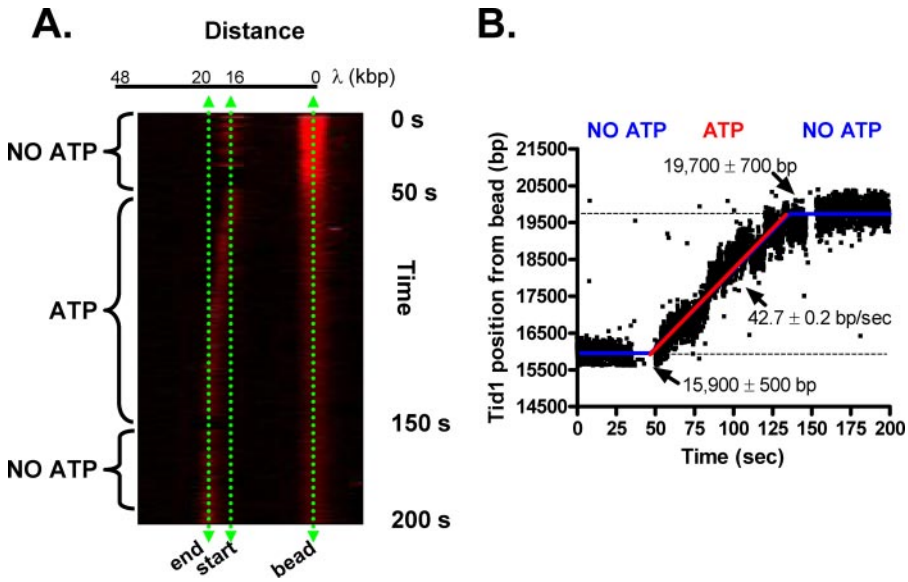

FIGURE 3. **Tid1 translocation requires ATP.** *A*, a kymograph depicting Tid1 translocation in the presence and absence of ATP. Tid1 translocation experiments were performed as described under "Experimental Procedures" with the exception that a three-channel flow cell was used. The trapped FITC-Tid1 bound to the λ DNA molecule was first moved to channel 2 without ATP and monitored for 50 s. To verify that the bound molecule is active, the DNA molecule was then moved to channel 3 with ATP and observed for 100 s. Finally, the same molecule was moved back to channel 2 and observed for another 50 s. The *vertical green arrows* mark the initial binding site of the FITC-Tid1 (*start*), the position of the molecule after translocation (*end*), and the position of the bead (bead). A schematic of the λ DNA is drawn at the *top* of the kymograph. *B*, graphical representation of the data in *A*. The position of Tid1 relative to the bead was plotted as a function of time. The translocation profile was fit to a three-segment line using Prism version 4. The initial and final binding positions and the velocity of translocation in the presence of ATP, along with their respective S.D. values, are indicated. (See Movie M3 for the video.)

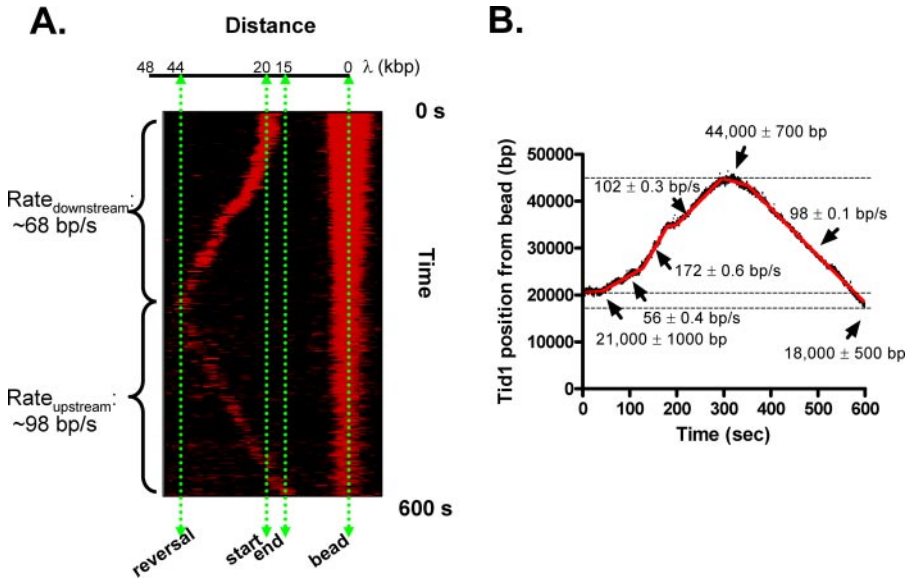

FIGURE 4. **Tid1 translocation can exhibit complex behavior.** *A*, a kymograph depicting a single Tid1 complex translocation showing a lag, a pause, velocity changes, and reversal of direction. The *vertical green arrows* mark the initial binding site of FITC-Tid1 (*start*), the reversal and a pause site (*reversal*), the position of the molecule after translocation (*end*), and the position of the bead (*bead*). A schematic of the λ DNA is drawn at the *top* of the kymograph. *B*, graphical representation of complex translocation. The position of Tid1 relative to the bead was plotted as a function of time. The translocation profile was fit to a multisegment line using Prism version 4. The initial and final binding positions, the position of the reversal, and the velocities of translocations, along with their respective S.D. values, are indicated. (See Movie M4 for the video.)

was ATP-dependent, the captured molecule was then moved back to the second channel and monitored for an additional 50 s. As expected, translocation ceased as soon as the molecule entered the solution lacking ATP, and the position of the complex remained unchanged at 19,700 ± 700 bp. Similar observations were made for 5 additional molecules (data not shown). These observations demonstrate the requirement for ATP during translocation.

Tid1 Translocation Can Exhibit Complex Behavior—In addition to the simple, monotonic behavior that was shown in Figs. 1 and 3, like Rad54 (20), we also observed complex translocation behavior (Table 1). Approximately one-third of the translocating complexes showed monotonic movement. The remaining two-thirds demonstrated complex translocation behavior that included intermittent pausing (28%) and changes in translocation direction (36%); for all (100%) of these "complex" FITC-Tid1 molecules, there were associated variations in velocity (data not shown).

Fig. 4 shows an example of a particularly complex FITC-Tid1 translocation, which displays pausing and a direction change as well as multiple translocation velocities. In this particular molecule, the initial binding position of FITC-Tid1 on the DNA was 21,000 ± 1,000 bp. Upon transferring the captured molecule into channel 2 containing ATP, the bound Tid1 molecule demonstrated downstream movement after a brief lag of about ~20 s; lags were also observed for Rad54 (20). The rate of translocation after the lag was initially slow but poorly defined (~56 bp/s) and then clearly switched to 172 ± 0.6 bp/s and was followed by a brief pause and then changed to 102 ± 0.3 bp/s. Afterward, the FITC-Tid1 was near the end of the λ DNA, whereupon the translocating complex paused briefly and reversed direction to move toward the bead (upstream) at a uniform rate of 98.3 ± 0.1 bp/s. We speculate that the translocation machinery consists of more than one Tid1 monomer, most probably a hexameric or dodecameric ring (21, 36, 37), and that the change of direction may be due to disengagement of one motor and reengagement of the other. The ability of Tid1 to translocate bidirectionally might be analogous to the behavior of RuvB protein, which is a dsDNA translocase from *Escherichia coli*

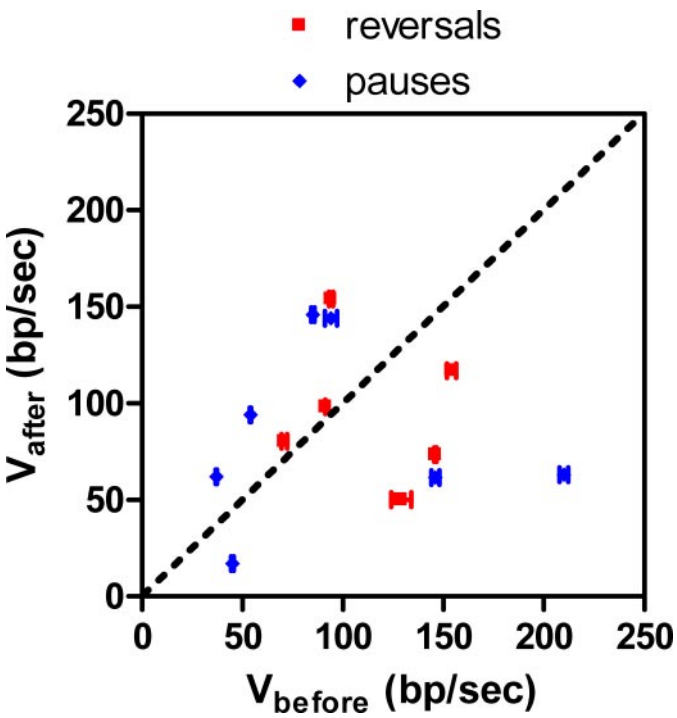

FIGURE 5. **Tid1 velocities before and after reversals/pauses are not correlated.** The translocation velocities before a pause or reversal are plotted against velocities after resumption of translocation or the change in translocation direction, respectively. The *diagonal line* represents the expected trend if rates before and after are correlated. The S.D. values are indicated by *error bars*. When error bars are not visible, the S.D. value was smaller than the size of the *symbols* used for the data points.

that promotes DNA branch migration. RuvB forms double hexameric rings around DNA, with the hexamers oriented in opposite directions. The consequence of this architecture is that, when RuvB is assembled with RecA at a four-way DNA junction with its partner protein RuvA, duplex DNA is pumped in opposing directions through this dodecameric structure (36, 38). If this analogy is apt, then if only one postulated Tid1 hexamer were engaged with the DNA at any one time, we could observe bidirectional translocation when translocation responsibility switched from one hexamer to the other. Our hypothesis is also supported by the fact that Tid1 translocation rates before and after pauses and reversals are largely uncorrelated (Fig. 5). If the same motor were translocating before and after pausing, then we would expect that the velocities would be similar and fall on the diagonal line. As stated above, for this reason, we feel that it is justified to consider each translocation segment as representing the behavior of a motor subunit that is engaged for the duration of that translocation event. However, if summed over all segments, the observed processivity of the FITC-Tid1 complex can be quite high; one molecule that reversed directions traveled 55,000 bp before dissociating (data not shown). Interestingly, the same behavior was seen for Rad54, highlighting another mechanistic similarity for these two motor proteins.

The Translocating Tid1 Can Dissociate Three-stranded Structures—Our data thus far provide evidence for the ability of Tid1 to move on dsDNA in an ATP-dependent fashion. To determine whether translocation by Tid1 on DNA can result in the displacement of bound objects, we tested whether Tid1 can dissociate three-stranded DNA structures using ensemble assays. Given that Rad54 can displace the non-Watson-Crick paired DNA strand of a triplex DNA structure (25), we tested the ability of Tid1 to displace the invading DNA strand of a recombination intermediate called a joint molecule or D-loop (6). The pairing of ssDNA with a region of homology in duplex DNA displaces the non-complementary strand, giving rise to a D-loop-shaped structure. The D-loop is a three-stranded DNA structure that can undergo branch migration, and given that Rad54 can accelerate the migration of both three- and four-stranded joint molecules (13, 14, 16), we were curious to know whether Tid1 also shared this capability. A D-loop substrate was formed *in vitro* using RecA protein to assimilate a complementary 100-mer ssDNA into supercoiled DNA, and then it was deproteinized and purified. Tid1, at increasing concentrations (0–400 nM), was added to the purified D-loops. As shown in Fig. 6, *A* and *B*, Tid1 could promote dissociation of the D-loops in a concentration-dependent manner. As expected, the loss of D-loops corresponded with an increase in the amount of the displaced 100-mer ssDNA. The time course for Tid1-catalyzed dissociation of D-loops is shown in Fig. 6*C*; Tid1 can completely dissociate the D-loops within 5 min.

Tid1 may catalyze displacement of the D-loops by two possible mechanisms: 1) by physically displacing the annealed 100-mer during translocation or 2) by altering the topology of the covalently closed duplex DNA (39), which would generate torsional constraints that would force the paired strand out of the duplex. To determine whether alterations in DNA topology contribute to unwinding, we tested the ability of Tid1 to unwind a second substrate, a linear joint molecule. Being linear, this joint molecule will not be intrinsically topological constrained; therefore, displacement of the paired ssDNA would largely be a consequence of translocation by Tid1. Fig. 6*D* compares the ability of the same amount of Tid1 to unwind linear joint molecules as well as D-loops. The data show that Tid1 can dissociate both structures, indicating that superhelicity-driven changes in DNA topology are not a requirement for Tid1-mediated dissociation of a joint molecule. Importantly, dissociation of linear joint molecules as well as D-loops fails to occur in the presence of ATPγS, a nonhydrolyzable analog of ATP, demonstrating the requirement for translocation in Tid1-mediated dissociation. We speculate that translocation by Tid1 removes impediments from its path by physically displacing them, a view that is consistent with the behavior and structure of its homolog, Rad54 (21, 40, 41).

Using a single molecule technique that was developed previously to study Rad54, we determined both the rate and processivity of Tid1 translocation on duplex DNA. Our values are in agreement with those reported recently (28). In that work, translocation of fluorescently labeled Tid1 (using anti-thioredoxin antibody coupled to quantum dots) was measured using total internal reflection fluorescence microscopy, a method that is complementary to our experimental strategy. Given the size of the quantum dot relative to the protein and the potential for interference from the surface, the quantitative agreement is

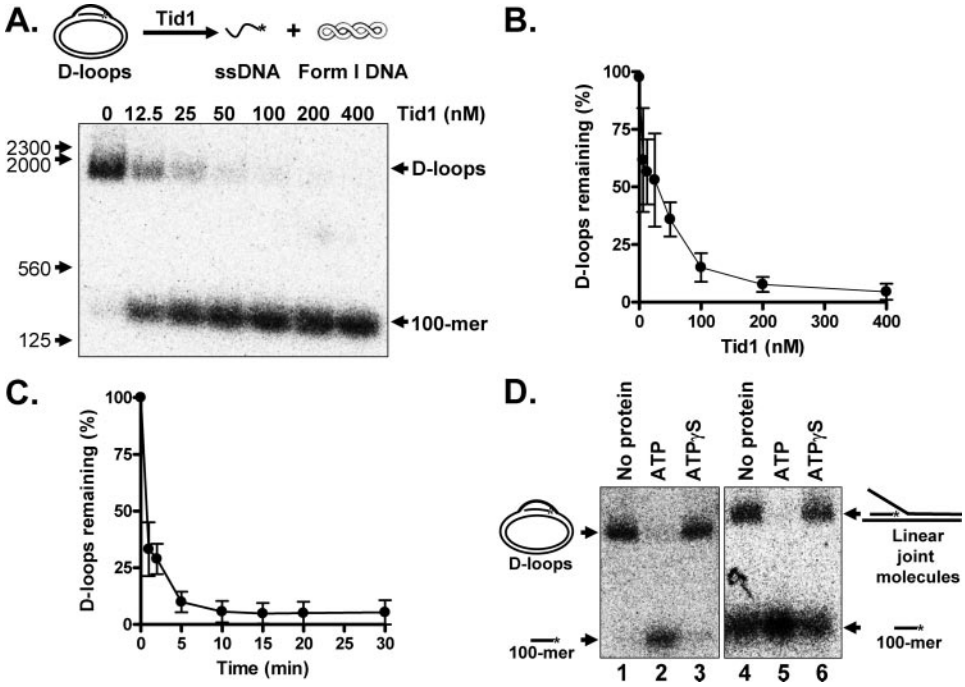

FIGURE 6. **Tid1 translocation leads to dissociation of joint molecule structures.** *A*, image of gel showing dissociation of D-loops (1.6 μM nt; 0.3 nM molecules) after a 30-min incubation as a function of Tid1 concentration (0–400 nM). A schematic of the reaction is drawn *above* the image. Positions of D-loops, free 100-mer, and markers are indicated. *B*, quantification of data from *A*. *C*, time course of Tid1-mediated (300 nM) dissociation of D-loops (1.6 μM nt; 0.3 nM molecules). The graphs were generated using Prism version 4. The percentage of D-loops remaining is the amount of D-loops present expressed as a percentage of the total signal (D-loops + released 100-mer). The *error bars* indicate experimental variation between at least four independent sets of experiments. *D*, unwinding of D-loops and linear joint molecules (1.6 μM nt; 0.3 nM molecules), demonstrating the requirement for ATP hydrolysis by Tid1 (300 nM). *Lane 1*, intact D-loops; *lanes 2* and *3*, unwinding of D-loops (15 min incubation) in the presence of ATP and ATPγS, respectively. *Lane 4*, intact linear joint molecules; *lanes 5* and *6*, unwinding of linear joint molecules (15-min incubation) in the presence of ATP and ATPγS, respectively. The positions of D-loops, linear joint molecules, and released 100-mer are indicated by schematic representations (not drawn to scale). The linear joint molecules contained a small amount of unincorporated 100-mer (*lane 4*). *Lanes 1–3* and *4–6* were analyzed on separate gels. The intensity of free 100-mer in *lane 5* was approximately equal to the sum of the two bands in *lane 4*.

comforting. In addition, those authors detected Tid1-mediated looping of DNA. Although we did not pursue the question of DNA looping here, we previously noted that Rad54 can also form DNA loops[5] (20). As we stated previously, it remains to be determined whether the DNA loops play an important role in the remodeling of protein-DNA complexes or whether translocation by the motor protein is sufficient.

Our work, which was conducted using both the same experimental method and reaction conditions as our prior examination of Rad54 (20), allows a direct comparison of Tid1 and Rad54 motor behavior. Tid1 translocates on DNA with a similar processivity (~10,000 bp) and complexity as Rad54, but with a ~2–4-fold lower speed. Interestingly, the observed rate of translocation (~80 bp/s) for Tid1 is comparable with the k_{cat} value for ATP hydrolysis determined from ensemble analysis (60 ATP/s for a Tid1 molecule).[4] If our Tid1 preparation is 100% active, then these results would suggest that for every bp translocated, Tid1 consumes one molecule of ATP; however, further experimentation is required to confirm this preliminary calculation.

We also demonstrated the capacity of Tid1 to migrate and dissociate three-stranded structures. This activity not only serves, at the very least, as a measure of the ability of Tid1 to displace, via translocation, a third DNA strand on duplex DNA, but may also reflect a biological function of this motor protein. The ability to translocate on DNA and move or remove impediments in its path, be it DNA, histones, or other proteins, is likely to be functionally significant, based on precedents established for its homolog, Rad54 (12–14, 16, 26, 42). However, as was shown and discussed for Rad54, the site of its action is targeted by the association of Rad54 with the Rad51-ssDNA complex (22, 23). Similarly, we imagine that Tid1 will be recruited to its sites of action by the association with its biological partner, Dmc1. Consequently, given their translocation similarities, we believe that the differentiation of Rad54 and Tid1 biological function will be determined largely by the specificity of their interactions with Rad51 and Dmc1, respectively. One can also imagine that this interaction may serve to both target and orient Tid1 and Rad54 in a translocation direction on duplex DNA that would be functionally productive, as in the case of the assembly of the dodecameric RuvB complex around the RuvA tetramer that binds to Holliday junctions (38). We further note that, although we used dissociation of three-stranded joint molecules here as a means to establish that translocation by Tid1 can remodel DNA, the use of longer joint molecules and the loading of Tid1 by Dmc1 into the region of DNA heteroduplex would have been manifest as DNA heteroduplex extension. In fact, Rad54 can branch migrate both the three- and four-stranded intermediates of DNA strand exchange (13, 14, 16). Interestingly, this behavior is again similar to that of RuvB. We find this analogy intriguing, and we believe that both Rad54 and Tid1 use their capacities to translocate along dsDNA to promote DNA heteroduplex extension. Furthermore, although analogy to RuvB is not proof, we also suggest that assembly of Rad54 or Tid1 around a Holliday junction in an opposed hexameric configuration could effect the Holliday junction migration as recently reported (16); because Holliday junctions are not present in our DNA substrates, we instead observe occasional bidirectional translocation by such proposed dodecameric (or equivalent) assemblies. Single molecule visualization, which is the only method that enables quantification of translocation behavior on dsDNA, together with other ensemble tools, should reveal more information in the

[5] I. Amitani and S. C. Kowalczykowski, unpublished observations.

future on the mechanism and function of these multifaceted motor proteins.

Acknowledgments—We are grateful to Dr. Wolf-Dietrich Heyer (University of California, Davis) for providing the expression strain (yWDH668), the expression plasmid (pWDH424), and invaluable suggestions. We thank Aura Carreira, Clarke Conant, Petr Cejka, Anthony Forget, Roberto Galletto, Jovencio Hilario, Ryan Jensen, Taeho Kim, Bian Liu, Edgar Valencia-Morales, Jody Plank, Behzad Rad, Alex Sica, and Jason Wong for comments on the manuscript.

REFERENCES

1. Dresser, M. E., Ewing, D. J., Conrad, M. N., Dominguez, A. M., Barstead, R., Jiang, H., and Kodadek, T. (1997) *Genetics* **147,** 533–544
2. Klein, H. L. (1997) *Genetics* **147,** 1533–1543
3. Shinohara, M., Shita-Yamaguchi, E., Buerstedde, J. M., Shinagawa, H., Ogawa, H., and Shinohara, A. (1997) *Genetics* **147,** 1545–1556
4. Cao, L., Alani, E., and Kleckner, N. (1990) *Cell* **61,** 1089–1101
5. Sun, H., Treco, D., Schultes, N. P., and Szostak, J. W. (1989) *Nature* **338,** 87–90
6. Kowalczykowski, S. C. (2000) *Trends Biochem. Sci.* **25,** 156–165
7. Masson, J. Y., and West, S. C. (2001) *Trends Biochem. Sci.* **26,** 131–136
8. Bishop, D. K., Park, D., Xu, L., and Kleckner, N. (1992) *Cell* **69,** 439–456
9. Shinohara, A., Ogawa, H., and Ogawa, T. (1992) *Cell* **69,** 457–470
10. Petukhova, G., Van Komen, S., Vergano, S., Klein, H., and Sung, P. (1999) *J. Biol. Chem.* **274,** 29453–29462
11. Petukhova, G., Sung, P., and Klein, H. (2000) *Genes Dev.* **14,** 2206–2215
12. Solinger, J. A., Kiianitsa, K., and Heyer, W. D. (2002) *Mol. Cell* **10,** 1175–1188
13. Solinger, J. A., and Heyer, W. D. (2001) *Proc. Natl. Acad. Sci. U. S. A.* **98,** 8447–8453
14. Solinger, J. A., Lutz, G., Sugiyama, T., Kowalczykowski, S. C., and Heyer, W. D. (2001) *J. Mol. Biol.* **307,** 1207–1221
15. Sugiyama, T., Kantake, N., Wu, Y., and Kowalczykowski, S. C. (2006) *EMBO J.* **25,** 5539–5548
16. Bugreev, D. V., Mazina, O. M., and Mazin, A. V. (2006) *Nature* **442,** 590–593
17. Eisen, J. A., Sweder, K. S., and Hanawalt, P. C. (1995) *Nucleic Acids Res.* **23,** 2715–2723
18. Lia, G., Praly, E., Ferreira, H., Stockdale, C., Tse-Dinh, Y. C., Dunlap, D., Croquette, V., Bensimon, D., and Owen-Hughes, T. (2006) *Mol. Cell* **21,** 417–425
19. Zhang, Y., Smith, C. L., Saha, A., Grill, S. W., Mihardja, S., Smith, S. B., Cairns, B. R., Peterson, C. L., and Bustamante, C. (2006) *Mol. Cell* **24,** 559–568
20. Amitani, I., Baskin, R. J., and Kowalczykowski, S. C. (2006) *Mol. Cell* **23,** 143–148
21. Kiianitsa, K., Solinger, J. A., and Heyer, W. D. (2006) *Proc. Natl. Acad. Sci. U. S. A.* **103,** 9767–9772
22. Mazin, A. V., Bornarth, C. J., Solinger, J. A., Heyer, W. D., and Kowalczykowski, S. C. (2000) *Mol. Cell* **6,** 583–592
23. Petukhova, G., Stratton, S., and Sung, P. (1998) *Nature* **393,** 91–94
24. Alexiadis, V., and Kadonaga, J. T. (2002) *Genes Dev.* **16,** 2767–2771
25. Jaskelioff, M., Van Komen, S., Krebs, J. E., Sung, P., and Peterson, C. L. (2003) *J. Biol. Chem.* **278,** 9212–9218
26. Alexeev, A., Mazin, A., and Kowalczykowski, S. C. (2003) *Nat. Struct. Biol.* **10,** 182–186
27. Singleton, M. R., and Wigley, D. B. (2002) *J. Bacteriol.* **184,** 1819–1826
28. Prasad, T. K., Robertson, R. B., Visnapuu, M. L., Chi, P., Sung, P., and Greene, E. C. (2007) *J. Mol. Biol.* **369,** 940–953
29. Kiianitsa, K., Solinger, J. A., and Heyer, W. D. (2002) *J. Biol. Chem.* **277,** 46205–46215
30. Mirshad, J. K., and Kowalczykowski, S. C. (2003) *Biochemistry* **42,** 5937–5944
31. Sambrook, J., Fritsch, E. F., and Maniatis, T. (1989) *Molecular Cloning: A Laboratory Manual*, 2nd Ed., pp. 1.42–1.45, Cold Spring Harbor Laboratory Press, Cold Spring Harbor, NY
32. Bianco, P. R., Brewer, L. R., Corzett, M., Balhorn, R., Yeh, Y., Kowalczykowski, S. C., and Baskin, R. J. (2001) *Nature* **409,** 374–378
33. McClure, W. R., and Chow, Y. (1980) *Methods Enzymol.* **64,** 277–297
34. Chi, P., Kwon, Y., Seong, C., Epshtein, A., Lam, I., Sung, P., and Klein, H. L. (2006) *J. Biol. Chem.* **281,** 26268–26279
35. Galletto, R., Amitani, I., Baskin, R. J., and Kowalczykowski, S. C. (2006) *Nature* **443,** 875–878
36. Stasiak, A., Tsaneva, I. R., West, S. C., Benson, C. J., Yu, X., and Egelman, E. H. (1994) *Proc. Natl. Acad. Sci. U. S. A.* **91,** 7618–7622
37. Massey, T. H., Mercogliano, C. P., Yates, J., Sherratt, D. J., and Lowe, J. (2006) *Mol. Cell* **23,** 457–469
38. Parsons, C. A., Stasiak, A., Bennett, R. J., and West, S. C. (1995) *Nature* **374,** 375–378
39. Ristic, D., Wyman, C., Paulusma, C., and Kanaar, R. (2001) *Proc. Natl. Acad. Sci. U. S. A.* **98,** 8454–8460
40. Thoma, N. H., Czyzewski, B. K., Alexeev, A. A., Mazin, A. V., Kowalczykowski, S. C., and Pavletich, N. P. (2005) *Nat. Struct. Mol. Biol.* **12,** 350–356
41. Durr, H., Korner, C., Muller, M., Hickmann, V., and Hopfner, K. P. (2005) *Cell* **121,** 363–373
42. Holzen, T. M., Shah, P. P., Olivares, H. A., and Bishop, D. K. (2006) *Genes Dev.* **20,** 2593–2604